Primary structural differences at residue 226 of deer and elk PrP dictate selection of distinct CWD prion strains in gene-targeted mice

Jifeng Bian[a,b,1], Jeffrey R. Christiansen[a,b,1], Julie A. Moreno[a,b], Sarah J. Kane[a,b], Vadim Khaychuk[a,b], Joseph Gallegos[a,b], Sehun Kim[a,b], and Glenn C. Telling[a,b,2]

[a]Prion Research Center, Colorado State University, Fort Collins, CO 80525; and [b]Department of Microbiology, Immunology and Pathology, Colorado State University, Fort Collins, CO 80525

Edited by Stanley B. Prusiner, University of California, San Francisco, CA, and approved May 7, 2019 (received for review March 7, 2019)

Although the unifying hallmark of prion diseases is CNS neurodegeneration caused by conformational corruption of host prion protein (PrP) to its infective counterpart, contagious transmission of chronic wasting disease (CWD) results from shedding of prions produced at high titers in the periphery of diseased cervids. While deer and elk PrP primary structures are equivalent except at residue 226, which is glutamate in elk and glutamine in deer, the effect of this difference on CWD pathogenesis is largely unknown. Using a gene-targeting approach where the mouse PrP coding sequence was replaced with elk or deer PrP, we show that the resulting GtE226 and GtQ226 mice had distinct kinetics of disease onset, prion conformations, and distributions of prions in the brains of diseased mice following intracerebral CWD challenge. These findings indicate that amino acid differences at PrP residue 226 dictate the selection and propagation of divergent strains in deer and elk with CWD. Because prion strain properties largely dictate host-range potential, our findings suggest that prion strains from elk and deer pose distinct risks to sympatric species or humans exposed to CWD. GtE226 and GtQ226 mice were also highly susceptible to CWD prions following intraperitoneal and oral exposures, a characteristic that stood in stark contrast to previously produced transgenic models. Remarkably, disease transmission was effective when infected mice were cohoused with naïve cagemates. Our findings indicate that gene-targeted mice provide unprecedented opportunities to accurately investigate CWD peripheral pathogenesis, CWD strains, and mechanisms of horizontal CWD transmission.

prions | gene targeting | chronic wasting disease | strains | species barriers

Prions are infectious proteins that are responsible for a group of related, fatal, and incurable mammalian neurodegenerative disorders, which continue to increase in variety in novel species. The emergence of bovine spongiform encephalopathy (BSE), and its zoonotic transmission as variant Creutzfeldt Jakob disease (vCJD) (1), highlight the substantial economic, political, and public health impacts of these disorders, and epitomize their unpredictable epidemiology and potential for interspecies transmission. Chronic wasting disease (CWD), a burgeoning epidemic of deer, elk, and other cervids is of particular concern (2). The unparalleled efficiency of its contagious transmission in wild as well as captive animals (3, 4) is related not only to extensive peripheralization and shedding of CWD prions during infection (5), but also to their seemingly unlimited environmental persistence (6). Both the geographic range of CWD and the number of naturally susceptible host species continue to increase. At the time of this writing, 26 states and three Canadian provinces report disease in farmed and free-ranging animals, with prevalence in some circumstances as high as 50% (2). Affected North American species include mule deer (*Odocoileus hemionus*), black-tailed deer (*Odocoileus hemionus columbianus*), white-tailed deer (*Odocoileus virginianus*), Rocky Mountain elk (*Cervus elaphus nelsoni*), North American elk (*Cervus canadensis*), and Shira's moose (*Alces alces shirasi*) (2). In recent years CWD has acquired global epidemic status. Following importation of subclinically diseased North American elk, CWD was inadvertently introduced to South Korea, where it subsequently spread to native red deer (*Cervus elaphus elaphus*), sika deer (*Cervus nippon*), and offspring of crosses between red and sika deer (7–9). In 2016 CWD was identified in free-ranging Norwegian reindeer (*Rangifer tarandus tarandus*), marking the first time the disease was detected in Europe, or in this species (10). Additional Norwegian cases were subsequently detected in European moose (*Alces alces alces*) (11) and red deer. CWD was detected in a moose from Finland in 2018 (http://www.dailyfinland.fi/national/4548/moose-dies-of-cwd-for-1st-time-in-finland) and in a moose from Sweden in 2019 (https://www.sva.se/en/animal-health/wildlife/map-of-chronic-wasting-disease-cwd).

An important aspect of prion diseases is their transmissibility. Exposure of individuals to prions from the same species results in fatal central nervous system (CNS) degeneration, typically with prolonged incubation periods. During this clinically silent phase, prion replication results from the conformational corruption of a host-encoded glycophoshphatidyl inositol-anchored sialoglycoprotein, referred to as the cellular prion protein (PrP^{C}), by its abnormally conformed and biochemically distinct counterpart, PrP^{Sc}, which constitutes the infectious agent (12). While transmission of

Significance

Our gene-targeting strategy addresses several critical issues relating to chronic wasting disease (CWD), a contagious, lethal neurodegenerative prion disease affecting wild as well as captive cervids, which poses an uncertain risk to humans. First, we show that residue 226, the sole primary structural difference between deer and elk prion protein, dictates the selection and propagation of different CWD strains. Because the strain properties of prions affect their host-range potential, these findings suggest that CWD from elk and deer pose distinct risks to humans and other species. Second, we show that these gene-targeted mice offer an unprecedented means to address distinctive aspects of CWD peripheral pathogenesis and horizontal transmission that are not afforded by previously generated transgenic mouse models.

Author contributions: G.C.T. designed research; J.B., J.R.C., J.A.M., S.J.K., V.K., J.G., and S.K. performed research; J.B. and G.C.T. analyzed data; and G.C.T. wrote the paper.

The authors declare no conflict of interest.

This article is a PNAS Direct Submission.

[1]J.B. and J.R.C. contributed equally to this work.

[2]To whom correspondence may be addressed. Email: glenn.telling@colostate.edu.

This article contains supporting information online at www.pnas.org/lookup/suppl/doi:10.1073/pnas.1903947116/-/DCSupplemental.

Published online May 30, 2019.

prion diseases from one species to another has been demonstrated repeatedly, it is generally a less efficient process. At the molecular level, the efficiency of interspecies prion transmission is governed by two predominant factors. First, transmission is facilitated by primary structural identity between PrP^{Sc} and the PrP^{C} conversion template expressed in the newly infected host (13). Underscoring this concept, multiple studies demonstrate that transgenic (Tg) expression of PrP from various species, typically in the absence of endogenous mouse PrP (14), eliminates the resistance of mice to prions from those species. Second, while they lack nucleic acids, prions share with conventional infectious agents the ability to propagate heritable strain phenotypes, the properties of which also influence the ability of prions to breach species barriers (15). Strain properties are operationally defined by differences in times to disease onset after prion exposure (incubation period), clinical signs, and the relative intensity and distribution of PrP^{Sc} and neuropathological lesions in the CNS (16). At the molecular level, these distinguishable and heritable strain characteristics are enciphered by distinct PrP^{Sc} conformations (17, 18). To reconcile the interactive effects of conformationally dictated strain properties with PrP sequence variations, the conformational selection model postulated that particular PrP^{C} primary structures are optimized to select and propagate distinct quasispecies from an ensemble of conformations produced during prion replication in an infected host (19). However, it is worth noting that this model appears to be incompatible with nonadaptive prion amplification, where certain interspecies transmissions do not entail emergence of new strains or conformational changes in PrP^{Sc}, but instead produce prions that replicate in the species of prion origination and not the new host (20).

Naturally occurring single amino acid PrP polymorphisms can have profound effects on prion disease susceptibility. For example, in humans, variation at PrP residue 129 dictates the propagation of distinct prion states, including those causing variant, sporadic, and iatrogenic forms of CJD (21). The PrP coding sequences of CWD-susceptible cervids are equivalent except at codon 226: deer express PrP^{C} with glutamine (Q) at this position (Q226-cervid PrP^{C}), while elk PrP^{C} contains glutamate (E) (E226-cervid PrP^{C}) (22), and the red deer PrP coding sequence is dimorphic (23). Whether differences at residue 226 influence the portfolio of selected strains in CWD-affected deer and elk and, by extension, whether the strain properties of prions causing CWD in deer are distinct from those causing CWD in elk is largely unknown.

We previously produced prototype CWD-susceptible $Tg(CerPrP)1536^{+/-}$ mice that overexpress Q226-cervid PrP^{C}, and $Tg(CerPrP\text{-}E226)5037^{+/-}$ mice overexpressing E226-cervid PrP^{C} (24, 25), referred to as $Tg1536^{+/-}$ and $Tg5037^{+/-}$. While problematic approaches for studying CWD in the natural host or poorly susceptible experimental animals were largely superseded by the development of these, and other similar Tg mice [reviewed in ref. 16], undefined influences of random transgene insertions (position effects), and the use of different transgene expression vectors to create each line were among the drawbacks that prevented a full assessment and understanding of the influence of amino acid differences at residue 226 on CWD pathogenesis. Moreover, while studies in $Tg1536^{+/-}$ indicated the existence of two predominant, naturally occurring CWD strains (26), subsequent findings in other Tg mice drew attention to the potential for artifactual effects of transgene overexpression and resultant aberrant strain mutation that potentially complicate studies designed to assess strain prevalence (27). Finally, while Tg mouse models designed to abrogate species barriers to foreign prions have been primarily engineered with disease outcomes in the CNS in mind, it is unclear whether—or to what extent—they also accurately recapitulate aspects of peripheral prion pathogenesis. This consideration is particularly important in the context of CWD, given the crucial importance of peripheral prion replication and shedding in the contagious transmission of CWD in natural host species (5).

To address these shortcomings, we employed a gene-targeting (Gt) strategy in which the coding sequence of the gene encoding mouse PrP, referred to as *Prnp*, was precisely replaced by homologous recombination in embryonic stem (ES) cells with elk or deer PrP coding sequences, resulting in mice referred to as $GtE226^{+/+}$ and $GtQ226^{+/+}$. While this approach was previously employed to elegantly address the effects of mouse PrP polymorphisms on prion pathogenesis (28), other previously generated Gt mice designed to abrogate species barriers to bovine and human prions were unexpectedly found to be poorly susceptible to BSE and CJD prions compared with their Tg counterparts (14, 29–37). In contrast, we show here that $GtE226^{+/+}$ and $GtQ226^{+/+}$ are fully susceptible to CWD prions from a range of diseased animals by a variety of inoculation routes. Because their genetic backgrounds are identical except at codon 226, and because they express equivalent, physiological levels of PrP^{C}, $GtE226^{+/+}$ and $GtQ226^{+/+}$ mice afforded the additional prospect of precisely determining the effects of variability at PrP residue 226 on CWD pathogenesis and strain selection. Finally, we investigated the proposal (38) that gene-targeting strategies provide an accurate means to model peripheral pathogenesis in prion diseases, this being the underlying feature of CWD that contributes to its unprecedented contagious transmission.

Results

Production and Characterization of Gt Mice Expressing Deer or Elk PrP^{C} under the Control of Mouse PrP Gene Regulatory Elements. Using ES cells from FVB mice, we developed two lines of Gt mice by direct replacement of the *Prnp* coding sequence with the corresponding elements from deer or elk PrP, which differ only at codon 226 (Fig. 1*A*). The resulting $GtE226^{+/+}$ and $GtQ226^{+/+}$ mice are homozygous for the targeted alleles that express elk (E226-cervid PrP^{C}) and deer (Q226-cervid PrP^{C}), respectively. Because deer and elk PrP expression in these circumstances is under the control of *Prnp* regulatory elements, $GtE226^{+/+}$ and $GtQ226^{+/+}$ mice produced equivalent, physiological levels of mRNA and E226-cervid PrP^{C} and Q226-cervid PrP^{C} (Fig. 1 *B* and *C*). Because they were engineered and maintained on an inbred FVB background, $GtE226^{+/+}$ and $GtQ226^{+/+}$ are syngeneic, except at codon 226 of the PrP^{C} coding sequence.

Amino Acid Variation at Residue 226 of Host Cervid PrP^{C} Affects Kinetics of CWD. To assess whether or not physiological expression of elk and deer PrP^{C} in mice conferred susceptibility to CWD prions, we challenged $GtE226^{+/+}$ and $GtQ226^{+/+}$ mice intracerebrally (ic) with prions isolated from the CNS of CWD-affected North American deer and elk. All intracerebrally inoculated Gt mice, referred to as $GtE226^{+/+}$(ic) and $GtQ226^{+/+}$(ic), developed disease (Table 1), and their brains accumulated cervid PrP^{Sc} (Figs. 2*A* and 3). The kinetics of disease onset was more rapid in $GtE226^{+/+}$(ic) than in $GtQ226^{+/+}$(ic) mice, resulting in isolate mean incubation times that were 20–38% shorter in $GtE226^{+/+}$(ic) mice (Table 1). When we assessed the collective responses of all intracerebrally inoculated Gt mice, the 262 ± 4 (±SEM) d mean time to disease onset in $GtE226^{+/+}$(ic) mice (n = 87) was 26% shorter ($P \leq 0.0001$) than the 355 ± 7 d mean time to disease in $GtQ226^{+/+}$(ic) mice (n = 69) (Fig. 2*C*). We also intracerebrally inoculated Gt mice with elk CWD prions that were previously passaged in $Tg5037^{+/-}$ mice (25). Like the ancestral 04-0306 CWD prions from which they originated, $Tg5037^{+/-}$-derived prions produced disease with a time to onset that was 28% faster ($P \leq 0.001$) in $GtE226^{+/+}$(ic) than in $GtQ226^{+/+}$(ic) mice (Table 1). We conclude that Gt mice expressing deer or elk PrP are highly susceptible to intracerebral challenge with CWD prions. Because their genetic backgrounds are otherwise identical, and because PrP^{C} expression is equivalent in both lines,

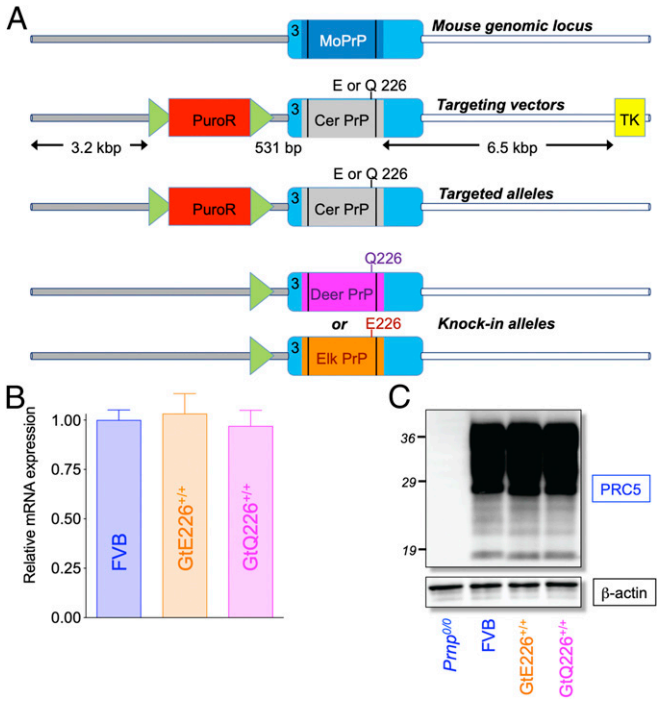

Fig. 1. Generation and characterization of Gt mice expressing cervid PrP^C. (*A*) Structure of the *Prnp* locus, targeting vectors, the targeted alleles, and resultant targeted *Prnp* loci after homologous recombination and removal of puromycin resistance gene, referred to as knockin alleles. Light blue rectangles designated number 3 represent *Prnp* exon 3 containing the complete PrP coding sequence, shown in dark blue for mouse PrP, gray for cervid (Cer) PrP and, more specifically, magenta and orange for deer and elk PrP, respectively, and the 3′UTR. The location of amino- and carboxyl-terminal signal peptidase cleavage sites are indicated as black vertical lines in coding sequences. In the targeting vectors, the puromycin resistance (PuroR) selection cassette (red box), flanked by loxP sites (green arrowheads), was inserted 531 nucleotides upstream of the deer or elk PrP translation initiation codons within intron 2 of *Prnp* (gray line). Targeting vectors contained an additional 3.2 kbs (kbp) of intronic sequence upstream of the floxed PuroR cassette. A thymidine kinase cassette was engineered 6.5-kbp distal to the coding sequences. The 5′ and 3′ homology arms of the targeting vectors were composed of FVB genomic sequences. (*B*) Levels of mRNA expression in brains of age-matched mice FVB (blue), $GtE226^{+/+}$ (orange), and $GtQ226^{+/+}$ (magenta) mice ($n = 3$ in each case) were determined by real-time quantitative reverse-transcription PCR using β-actin as an internal control. (*C*) Western blot analysis of PrP^C expressed in the brains of $GtE226^{+/+}$ and $GtQ226^{+/+}$ mice compared with FVB/N mice using mAb PRC5 (57). $Prnp^{0/0}$ knockout mice maintained on an inbred FVB background (41) served as a negative control. The position of protein molecular weight standards at 36, 29, and 19 kDa are shown.

we ascribe differences in the kinetics of disease onset in $GtQ226^{+/+}$ and $GtE226^{+/+}$ mice to the effects of amino acid variation at PrP^C residue 226.

We questioned whether the rapid and uniform induction of disease in $GtE226^{+/+}$ and $GtQ226^{+/+}$ mice reflected idiosyncratically virulent properties of CWD prions. Arguing against this notion, when we challenged $GtE226^{+/+}$ and $GtQ226^{+/+}$ mice with cervid prions from the CNS of diseased $Tg1536^{+/-}$ mice infected with either sheep SSBP/1 prions or mouse-adapted Rocky Mountain Laboratory (RML) scrapie prions (39, 40), all inoculated $GtE226^{+/+}$ mice developed disease with ∼250–260 mean incubation times that were comparable to those produced by CWD isolates (Table 1). In contrast to CWD prion transmissions, the mean incubation time of cervid-adapted SSBP/1 prions was more rapid in $GtQ226^{+/+}$ than in $GtE226^{+/+}$ mice. We conclude that $GtQ226^{+/+}$ and $GtE226^{+/+}$ mice are susceptible to different cervid prion strains, and that amino acid variation at residue 226 has distinct effects on the propagation of CWD and cervid-adapted scrapie prions.

To assess the consequences of codon 226 heterozygosity found naturally in red deer, we bred $GtE226^{+/+}$ with $GtQ226^{+/+}$ mice, and intracerebrally challenged the resulting heterozygous F_1 offspring, referred to as GtE/Q226(ic), with CWD prions. The mean incubation times of deer CWD isolates D10 and Db99 in GtE/Q226(ic) were equivalent to their relatively short incubation times in $GtE226^{+/+}$ ($P = 0.2$–0.7), but distinct from their longer mean incubation times in $GtQ226^{+/+}$ mice ($P < 0.05$). In contrast, the mean incubation times of elk CWD isolates 99W12389 and 001-44720 in GtE/Q226(ic) were intermediate between those registered in $GtE226^{+/-}$(ic) and $GtQ226^{+/-}$(ic) mice, producing incubation times that were distinct from those registered in $GtE226^{+/+}$ mice ($P < 0.0001$ to <0.01) (Table 1).

CWD Onset Is Inversely Related to Cervid PrP^C Expression in Intracerebrally Challenged Gt and Tg Mice. The use of the inbred FVB background to produce Gt mice expressing physiological levels of deer or elk PrP, as well as previously characterized $Tg1536^{+/-}$ and $Tg5037^{+/-}$ mice overexpressing deer or elk PrP, respectively (24, 25), allowed us to assess the effects of primary structural differences at residue 226 on the kinetics of CWD onset over a range of cervid PrP^C expression in a defined genetic context. We compared the responses of Tg and Gt mice challenged with matched CWD inocula, with the exception of isolate D92 which was only transmitted to Tg mice (Table 1 and *SI Appendix*, Table S1). The collective 264 ± 7 d mean incubation time resulting from intracerebral challenge of $Tg1536^{+/-}$ mice [$Tg1536^{+/-}$(ic)] ($n = 60$), which overexpress Q226-cervid PrP^C in the CNS at levels ∼fivefold higher in wild-type mice (24), was 24% shorter ($P \leq 0.0001$) than the 347 ± 8 d mean time to disease in $GtQ226^{+/+}$(ic) mice ($n = 46$). Similarly, the collective 204 ± 10 d mean incubation time in $Tg5037^{+/-}$(ic) mice ($n = 53$), which overexpress E226-cervid PrP^C in the CNS at levels ∼fivefold higher in wild-type mice (25), was 20% shorter ($P \leq 0.0001$) than the 256 ± 5 d mean time to disease in $GtE226^{+/+}$(ic) mice ($n = 52$). Consistent with our findings that disease occurred more rapidly in $GtE226^{+/+}$(ic) than $GtQ226^{+/+}$(ic) mice, the collective 204 ± 10 mean time to disease onset in $Tg5037^{+/-}$(ic) mice ($n = 53$) was 23% shorter ($P \leq 0.0001$) than the collective 264 ± 7 mean incubation time in $Tg1536^{+/-}$(ic) mice ($n = 60$) (Fig. 2*B* and *SI Appendix*, Table S1). Our use of a consistent inbred background and equivalent prion inocula allow us to conclude that the ∼20–25% more rapid mean incubation times in intracerebrally inoculated Tg mice compared with intracerebrally inoculated Gt mice, matched at residue 226, results from ∼fivefold higher transgene expression in Tg mice.

The availability of $Prnp^{0/0}$ knockout mice maintained on an inbred FVB background (41) allowed us to generate haploinsufficient counterparts of $GtE226^{+/+}$ and $GtQ226^{+/+}$ mice, referred to as $GtE226^{+/-}$ and $GtQ226^{+/-}$, and an additional means to assess the effects of cervid PrP^C expression on CWD incubation times in a controlled genetic context. All intracerebrally challenged $GtE226^{+/-}$ and $GtQ226^{+/-}$ mice, referred to as $GtE226^{+/-}$(ic) and $GtQ226^{+/-}$(ic), developed disease (Fig. 2*B* and Table 1), and accumulated PrP^{Sc} in the CNS (Fig. 2*A*). The collective 454 ± 7 d mean incubation time of $GtQ226^{+/-}$(ic) mice ($n = 26$) was 32% longer ($P \leq 0.0001$) than the 344 ± 11 mean time to disease in $GtQ226^{+/+}$(ic) mice ($n = 30$) receiving the same isolates, while the collective 379 ± 8 d mean incubation time in $GtE226^{+/-}$(ic) mice ($n = 23$) was 47% longer ($P \leq 0.0001$) than the 258 ± 6 mean time to disease in similarly challenged in $GtE226^{+/+}$(ic) mice ($n = 42$) (Fig. 2*B*). In support of the effects of residue 226 on the kinetics of disease onset, the mean time to disease onset was 17% shorter in $GtE226^{+/-}$(ic) than $GtQ226^{+/-}$(ic) mice ($P \leq 0.0001$) (Fig. 2*B*). Collectively, our findings in Tg and

Table 1. Disease susceptibility of Gt mice expressing elk or deer PrP following intracerebral inoculation with cervid prions

	Mean incubation times (d), ±SEM (n/n_o)							
	GtE226$^{+/+}$		GtQ226$^{+/+}$		Δt	GtE226$^{+/-}$	GtQ226$^{+/-}$	GtE/Q226
Inoculum	Primary	Secondary	Primary	Secondary	Primary	Primary	Primary	Primary
Elk CWD								
99W12389	225 ± 5 (10/10)	184 ± 6 (7/7)	361 ± 14 (6/6)		38% (<0.0001)	376 ± 8 (8/8)	461 ± 15 (7/7)	303 ± 4 (6/6)
01-0306	238 ± 7 (7/7)		305 ± 24 (7/7)		22% (<0.05)			
04-0306	251 ± 4 (7/7)	184 ± 7 (8/8)	331 ± 12 (9/9)		24% (<0.0001)	417 ± 19 (5/5)	480 ± 14 (5/5)	
012-09442	232 ± 8 (9/9)		338 ± 8 (6/6)		31% (<0.0001)			
001-44720	306 ± 11 (7/7)		405 ± 22 (7/7)		24% (<0.01)			360 ± 10 (4/4)
Red deer	222 ± 6 (8/8)		339 ± 6 (6/6)		35% (<0.0001)			
Deer CWD								
D10	284 ± 6 (12/12)		353 ± 30 (5/5)	332 ± 17 (5/5)	20% (<0.01)	351 ± 8 (5/5)	437 ± 18 (7/7)	296 ± 6 (9/9)
Db99	264 ± 12 (13/13)	221 ± 3 (9/9)	340 ± 26 (10/10)		22% (<0.01)	375 ± 17 (5/5)	448 ± 8 (7/7)	256 ± 15 (7/7)
978-24384	295 ± 5 (8/8)		385 ± 7 (7/7)		23% (<0.0001)			
001-39697	324 ± 4 (6/6)		407 ± 17 (6/6)		20% (<0.001)			
Total CWD	262 ± 4 (87/87)		355 ± 7 (69/69)		26% (<0.0001)	379 ± 8 (23/23)	454 ± 7 (26/26)	297 ± 8 (26/26)
Adapted prions								
04-0306 (*Tg5037*$^{+/-}$)	223 ± 8 (6/6)		308 ± 18 (5/5)		28% (<0.001)			
SSBP/1 (*Tg1536*$^{+/-}$)	246 ± 6 (6/6)		168 ± 3 (8/8)		−46% (<0.0001)			
RML (*Tg1536*$^{+/-}$)	260 ± 4 (8/8)							

Time to disease onset (incubation time) is expressed as the mean time, in days, at which inoculated mice first developed ultimately progressive signs of neurological disease. Variance is expressed as ±SEM. n/n_o, number of diseased mice/number of inoculated mice. Mice dying of unrelated intercurrent illnesses were excluded from these calculations. 04-0306 (*Tg5037*$^{+/-}$), prions from the brains of diseased Tg5037$^{+/-}$ mice infected with isolate 04-0306. Primary refers to passage of CWD isolates to Gt mice; secondary refers to serial passage of prions in brain homogenates of diseased mice from primary transmission of those isolates to mice of the same genetic constitution. Δt, percent difference in mean incubation time of individual isolates in GtE226$^{+/+}$ compared with GtQ226$^{+/+}$ mice expressed as the extent to which incubation times are more rapid in GtE226$^{+/+}$ mice. *P* values of differences, calculated by Student's *t* test are shown in brackets. Total CWD, aggregate values of all CWD diseased animals in each genotype.

Gt mice demonstrate that CWD incubation times following intracerebral inoculation are inversely related to levels of CNS cervid PrP^{C} expression in the host. Accordingly, incubation times of CWD prions in Tg5037$^{+/+}$(ic) mice, which are homozygous for the transgene array, were 23% more rapid than in counterpart hemizygous Tg5037$^{+/-}$ mice (Fig. 2*B*). Moreover, the reproducibly more rapid time to disease in mice expressing E226-cervid PrP^{C} compared with their counterparts expressing Q226-cervid PrP^{C} across a range of transgene expression underscores the consistent impact of residue 226 on the kinetics of CWD.

Amino Acid Variation at Residue 226 of PrP^{Sc} Influences the Properties of CWD Prions. In light of the effects of residue 226 on the kinetics of disease onset, we sought to define differences in the characteristics of E226-cervid PrP^{Sc} and Q226-cervid PrP^{Sc} constituting E226 and Q226 prions produced in the CNS of intracerebrally challenged Gt mice. Although the electrophoretic migration patterns, and proportions of di-, mono-, and a-glycosyl forms of E226-cervid PrP^{Sc} and Q226-cervid PrP^{Sc} from GtE226$^{+/+}$(ic) and GtQ226$^{+/+}$(ic) mice were indistinguishable (Fig. 2*A*), they exhibited distinctive denaturation profiles following treatment with a range of guanidinium hydrochloride (GdnHCl) concentrations before digestion with proteinase K (PK) (42) (Fig. 2*D*). The 2.10 M concentration of GdnHCl producing half-maximal denaturation ($GdnHCl_{1/2}$) of E226-cervid PrP^{Sc} from the CNS of diseased GtE226$^{+/+}$ mice was distinct from the 2.52 M $GdnHCl_{1/2}$ value of Q226-cervid PrP^{Sc} ($P \leq 0.0001$) produced in the CNS of GtQ226$^{+/+}$ mice. In addition, the unfolding characteristics of PrP^{Sc} produced in the brains of heterozygous GtE/Q226(ic) mice, and the resultant 2.30 M $GdnHCl_{1/2}$ were distinct from, and intermediate between those of E226-cervid PrP^{Sc} and Q226-cervid PrP^{Sc}. These results indicate that residue 226 influences the conformational properties of CWD prions; and that the conformation of CWD-derived Q226-cervid PrP^{Sc} is more stable to denaturation than that of CWD-derived E226-cervid PrP^{Sc}.

We used histoblotting (43) and immunohistochemical (IHC) analysis to assess cervid PrP^{Sc} distribution in the brains of diseased intracerebrally inoculated Gt mice (Fig. 3). Infection of GtQ226$^{+/+}$(ic) mice with either E226 (Fig. 3*A*) or Q226 (Fig. 3*B*) CWD prions resulted in a relatively disorganized distribution of Q226-cervid PrP^{Sc} characterized by intensely staining asymmetric deposits throughout the cortex, hippocampus, thalamus, and hypothalamus (Fig. 3*I*) that were consistently ipsilateral to the inoculation site. In contrast, the CNS of CWD-infected GtE226$^{+/+}$(ic) mice exhibited two distinct patterns of E226-cervid PrP^{Sc} deposition, depending on whether disease resulted from infection with either E226 or Q226 CWD prions. In E226 CWD prion-infected GtE226$^{+/+}$(ic) mice, E226-cervid PrP^{Sc} distribution was relatively diffuse, and bilaterally symmetrical in cortical, thalamic, and hypothalamic regions (Fig. 3 *C*, *D*, and *J*), whereas in GtE226$^{+/+}$(ic) mice receiving Q226 CWD prions, E226-cervid PrP^{Sc} was asymmetrically deposited in the thalamus, again ipsilateral to the inoculation site, with relative sparing of cortical and hippocampal regions (Fig. 3 *E*, *F*, and *K*). Patterns of PrP^{Sc} deposition in the CNS of CWD infected heterozygous GtE/Q226(ic) mice (Fig. 3 *G*, *H*, and *L*) more closely resembled the asymmetrical, disorganized patterns of PrP^{Sc} in the CNS of diseased GtQ226$^{+/+}$(ic) mice than the symmetrically diffuse PrP^{Sc} pattern in GtE226$^{+/+}$(ic) mice. In GtE226$^{+/-}$(ic) mice, E226-cervid PrP^{Sc} deposition patterns (Fig. 3 *Q* and *R*) were comparable to, but less intense than E226-cervid PrP^{Sc} found in the cortex, hippocampus, thalamus, and hypothalamus of homozygous GtE226$^{+/+}$(ic) mice (Fig. 3*J*), while in CWD-infected haploinsufficient Gt226Q$^{+/-}$

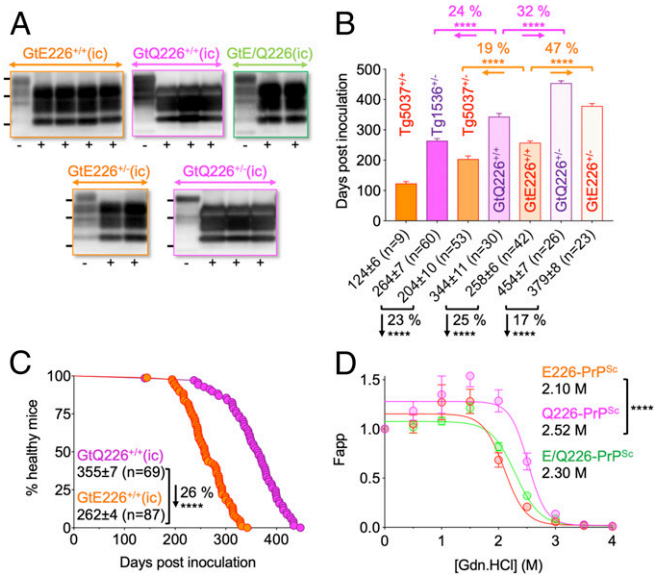

Fig. 2. The effects of cervid PrP residue 226 and cervid PrP^C expression on the kinetics of disease onset and CNS PrP^{Sc} accumulation following intracerebral challenge with CWD. (*A*) Western immunoblots of PrP in the CNS of diseased Gt mice intracerebrally inoculated with CWD prions. (*Upper*) $Gt^{+/+}$ mice; (*Lower*) $Gt^{+/-}$ mice. Samples were either untreated (25 μg) or treated (100 μg) with PK as indicated, and immunoblots were probed with mAb PRC5. The positions of protein molecular weight standards at 36, 29, and 19 kDa are shown. (*B*) Time to disease onset in intracerebrally challenged Gt and Tg mice expressing either E226-PrP^C (orange) or Q226-PrP^C (magenta) is proportional to levels of PrP^C expressed in the CNS. $Tg5037^{+/-}$ and $Tg1536^{+/-}$ mice express transgene-encoded PrP^C in the hemizygous state; $Tg5037^{+/+}$ are homozygous for the transgene array. (*C*) Differences at residue 226 of deer and elk PrP^C affect the tempo of disease onset in intracerebrally inoculated Gt mice. Time to disease onset of CWD inoculated $GtE226^{+/+}$ (orange), and $GtQ226^{+/+}$ (magenta) following intracerebral challenge. Curves represent the aggregate responses of all CWD inocula used to challenge Gt mice in Table 1. In *B* and *C*, aggregate incubation times of multiple CWD isolates are expressed as mean ± SEM, as well as the number (*n*) of diseased mice, with significance determined using Student's *t* test. $^{****}P \leq 0.0001$. (*D*) Resistance of PrP^{Sc} in the brains of diseased, intracerebrally inoculated Gt mice to PK following treatment with varying concentrations of GdnHCl. Immunoblots were probed with mAb PRC5. Brain extracts from $GtE226^{+/+}$ (orange), $GtQ226^{+/+}$ (magenta), and GtE/Q226 (green). Each point is the mean value derived from the analysis of eight diseased mouse brains, and error bars correspond to the SD of those mean values. Fapp, fraction of apparent PrP^{Sc} (maximum signal-individual signal)/(maximum signal-minimum signal). Sigmoidal dose–response curves were plotted using a four-parameter algorithm and nonlinear least-square fit. Statistical differences between the concentrations of GdnHCl producing half-maximal PrP^{Sc} denaturation were calculated. $^{****}P \leq 0.0001$.

(ic) mice (Fig. 3 *S* and *T*), Q226-cervid PrP^{Sc} deposition patterns resembled the disorganized amalgamations of aggregates found in the cortex, hippocampus, thalamus, and hypothalamus of their diseased homozygous $GtQ226^{+/+}$(ic) counterparts (Fig. 3*I*). We conclude that residue 226 influences the targeted accumulation of cervid PrP^{Sc} in the CNS following intracerebral infection of Gt mice.

We performed serial transmissions of CWD prions produced in the brains of diseased Gt mice to additional Gt mice by intracerebral inoculation (Table 1). The relatively disorganized pattern of Q226-cervid PrP^{Sc} aggregates in the cortex, hippocampus, thalamus, and hypothalamus observed upon primary transmission of Q226 CWD prions to $GtQ226^{+/+}$(ic) mice (Fig. 3 *A*, *B*, and *I*) was maintained when the resulting Q226 prions were passaged to additional $GtQ226^{+/+}$(ic) mice (Fig. 3*M*). Similarly, the widespread, diffuse granular deposition of E226-cervid PrP^{Sc} in the cortex, hippocampus, and thalamus observed upon primary transmission of E226 CWD prions to $GtE226^{+/+}$(ic) mice (Fig. 3 *C*, *D*, and *J*) was preserved upon serial passage of the resulting E226 prions to additional $GtE226^{+/+}$(ic) mice (Fig. 3 *N* and *O*). However, the restricted, bilaterally asymmetrical thalamic pattern of E226-cervid PrP^{Sc} produced upon primary transmission of Q226 CWD prions to $GtE226^{+/+}$(ic) mice (Fig. 3 *E*, *F*, and *K*) was not sustained when the resulting E226 prions were serially passaged to $GtE226^{+/+}$(ic) mice (Fig. 3*P*). Instead, the new E226-cervid PrP^{Sc} pattern corresponded to the widespread, diffuse granular pattern of E226-cervid PrP^{Sc} produced upon primary transmissions of E226 CWD prions to $GtE226^{+/+}$(ic) mice (Fig. 3 *C*, *D*, and *J*). These findings provide further support for the notion that cervid PrP^{Sc} accumulation in Gt mice is dictated by the effects of residue 226 in host-expressed cervid PrP^C.

Susceptibility of Gt Mice to Peripheral Challenge. We investigated the responses of Gt mice to CWD prions introduced by the intraperitoneal (ip) and oral (po) routes, referred to as Gt(ip) and Gt(po). Gt(ip) and (po) mice developed prion disease (Fig. 4 *A* and *B* and Table 2) and accumulated PrP^{Sc} in the CNS (Figs. 4*E* and 5). The collective 315 ± 3 d mean incubation time of all inoculated $GtE226^{+/+}$(ip) mice ($n = 58$) was 14% shorter ($P \leq 0.0001$) than the 367 ± 13 d mean incubation time of all $GtQ226^{+/+}$(ip) mice ($n = 22$) (Fig. 4 *A* and *B*), indicating that the residue 226 dimorphism affected the kinetics of CWD onset following intraperitoneal as well as intracerebral challenge.

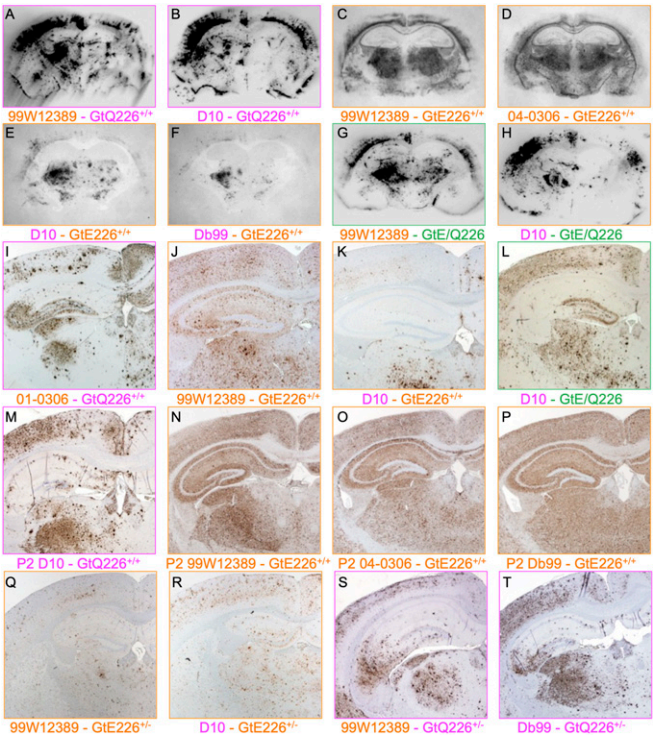

Fig. 3. PrP^{Sc} distribution in brains of diseased Gt mice intracerebrally challenged with CWD prions. For consistency, coronal sections through the hippocampus and thalamus are shown in all cases. (*A–H*) PK-treated histoblots probed with mAb PRC5. (*I–T*) Immunohistochemical analysis with Fab D18. (Magnification: 2×.) (*A–L*) Primary transmissions of CWD isolates from deer or elk to either $GtE226^{+/+}$ (orange), $GtQ226^{+/+}$ (magenta), or heterozygous GtE/Q226 (green). (*Q–T*) Primary transmissions of CWD isolates from deer or elk to either hemizygous $GtE226^{+/-}$ or $GtQ226^{+/-}$. (*M–P*) Secondary transmissions (P2) of CWD prions, originally passaged in $GtE226^{+/+}$ (inoculum designated in orange) or $GtQ226^{+/+}$ (inoculum designated in magenta).

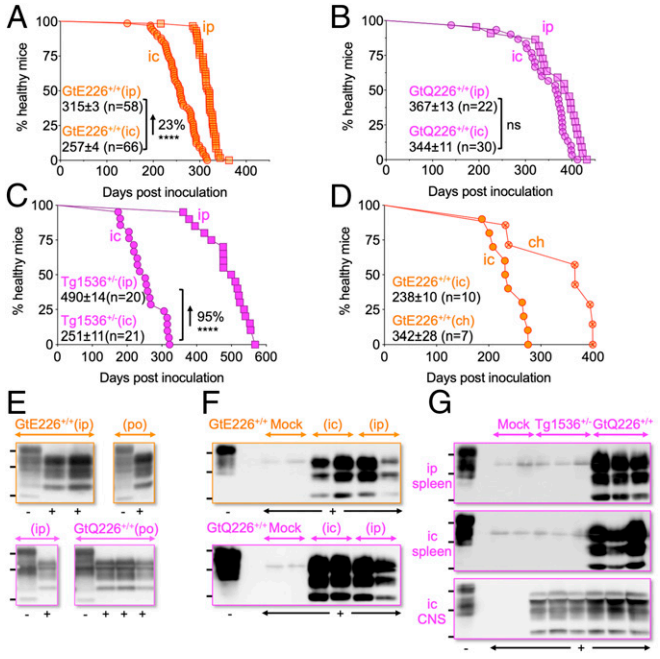

Fig. 4. Response of Gt and Tg mice expressing cervid PrP^C to peripheral challenges with CWD prions. (*A* and *B*) Aggregate responses of intraperitoneally challenged (squares) $GtE226^{+/+}$ (orange), $GtQ226^{+/+}$ (magenta) following CWD inoculation with isolates from Table 2, compared with intracerebrally inoculated mice (circles) challenged with the same isolates (Table 1). (*C*) Aggregate responses of intraperitoneally challenged $Tg1536^{+/-}$ mice (magenta squares) compared with intracerebrally inoculated $Tg1536^{+/-}$ mice (circles) challenged with the same isolates. Incubation times are expressed as mean ± SEM, as well as the number (*n*) of diseased mice with significant differences determined using Student's *t* test. $^{****}P \leq 0.0001$; ns, not significant ($P > 0.05$). (*D*) Time to disease onset in $GtE226^{+/+}$ mice intracerebrally inoculated with elk isolate 99W12389 (orange circles) and cohoused (ch) uninoculated $GtE226^{+/+}$ mice (orange crossed circles). (*E*) Immunoblots of PrP in the CNS of diseased Gt mice intraperitoneally (ip) or orally (po) inoculated with CWD prions. (*F*) Immunoblots showing PrP^{Sc} accumulation in the spleens of diseased $GtE226^{+/+}$ (orange, *Upper*), and $GtQ226^{+/+}$ mice (magenta, *Lower*) following intracerebral and intraperitoneal challenge, compared with age matched mock-infected mice. (*G*) Western immunoblots showing PrP^{Sc} accumulation in the spleens of diseased $GtQ226^{+/+}$ mice but not $Tg1536^{+/-}$ mice that were intraperitoneally inoculated (*Top*) or intracerebrally inoculated (*Middle*) with CWD prions, compared with mock infected, age matched $GtQ226^{+/+}$ mice. PrP^{Sc} was detected in brain extracts of diseased $Tg1536^{+/-}$ mice that failed to accumulate PrP^{Sc} in spleens (*Bottom*). In *F* and *G*, Western blots of 100-μg spleen tissues not treated with PK (–), and 1 mg treated with PK (+) were probed with mAb PRC5. The positions of protein molecular mass standards of 36, 29, 19 kDa, from top to bottom, are shown.

When we compared the kinetics of disease onset following inoculation by the intracerebral and intraperitoneal routes, the collective 315 ± 3 d mean incubation time of $GtE226^{+/+}$(ip) mice was 23% longer than the 257 ± 4 d ($n = 66$) time to disease in $GtE226^{+/+}$(ic) mice receiving the same inocula ($P \leq 0.0001$) (Fig. 4*A*). This outcome is in accordance with previous studies of scrapie prion transmissions in rodent models that have consistently demonstrated a protracted time to disease onset following intraperitoneal compared with intracerebral challenge (44). We were therefore surprised to detect no difference ($P > 0.05$) in the collective 367 ± 13 mean time to CWD onset in $GtQ226^{+/+}$(ip) mice ($n = 22$) compared with the collective 344 ± 11 mean time to disease of $GtQ226^{+/+}$(ic) mice ($n = 30$) inoculated with the same isolates (Fig. 4*B*).

To explore this finding further, we compared the responses of $Tg1536^{+/-}$ mice to CWD challenges by the intracerebral and intraperitoneal routes. While the collective mean incubation time of $Tg1536^{+/-}$(ic) mice challenged with three CWD isolates was 251 ± 11 d ($n = 21$), $Tg1536^{+/-}$(ip) mice receiving the same isolates failed to register disease until after 490 ± 14 d ($n = 20$), which was a 95% prolongation of disease onset compared with $Tg1536^{+/-}$(ic) mice ($P \leq 0.0001$) (Fig. 4*C*), and a 34% extension compared with $GtQ226^{+/+}$(ip) mice (Fig. 4 *B* and *C*). While the spleens of diseased $GtE226^{+/+}$ and $GtQ226^{+/+}$ mice accumulated PrP^{Sc} following intraperitoneal or intracerebral inoculation (Fig. 4*F*), only the CNS but not the spleens of CWD inoculated $Tg1536^{+/-}$ mice accumulated PrP^{Sc} after either intracerebral or intraperitoneaal challenges (Fig. 4*G*). We conclude that the more efficient disease induction in $GtQ226^{+/+}$(ip) than $Tg1536^{+/-}$(ip) mice is the consequence of more accurate control of peripheral cervid PrP^C expression by *Pmp* regulatory elements in Gt mice.

Consistent with previous studies, which established that the oral route of prion infection is less efficient than either the intraperitoneal or intracerebral routes (45), incubation times of CWD isolates in Gt(po) mice were generally longer than the corresponding Gt(ic) and Gt(ip) transmissions, and attack rates were not always uniformly complete (Table 2). However, in those mice that did develop disease, the 366 ± 26 aggregate time to disease onset in $GtE226^{+/+}$(po) mice ($n = 17$) was 23% faster ($P \leq 0.001$) than the 474 ± 19 mean time to onset in $GtQ226^{+/+}$(po) mice ($n = 18$).

Properties of Prions Produced in the Brains of Peripherally Challenged Gt Mice. Histoblotting and IHC analyses demonstrated that cervid PrP^{Sc} in the brains of diseased Gt(ip) and Gt(po) mice accumulated as bilaterally symmetrical deposits in cortical and thalamic regions, with relative sparing of the hippocampus (Fig. 5). The general pattern of PrP^{Sc} deposition in the CNS of CWD infected Gt(ip) and Gt(po) mice was different from the patterns of PrP^{Sc} accumulation in the brains of diseased Gt(ic) mice (Fig. 3). Although patterns of PrP^{Sc} accumulation in $GtQ226^{+/+}$(ic) and $GtE226^{+/+}$(ic) mice receiving E226 CWD prions were recognizably different from the patterns resulting from Q226 CWD prion infection (Fig. 3), these distinctions were not obvious upon evaluation of $GtE226^{+/+}$(ip) and $GtQ226^{+/+}$(ip) mice, nor when comparing $GtE226^{+/+}$(po) with $GtQ226^{+/+}$(po) mice (Fig. 5).

When we intracerebrally challenged $GtE226^{+/+}$ mice with prions from the CNS of diseased $GtE226^{+/+}$(ip) mice inoculated with the 99W12389 elk CWD isolate, mean incubation times in the resulting diseased mice, referred to as $GtE226^{+/+}$(ip-ic), decreased from ∼300 d in $GtE226^{+/+}$(ip) to ∼200 d (Table 2), which was similar to the mean incubation time upon primary transmission of this isolate to $GtE226^{+/+}$(ic) mice (Table 1). Additionally, whereas the pattern of E226-cervid PrP^{Sc} deposition in the CNS of diseased $GtE226^{+/+}$(ip) (Fig. 5*A*) was distinct from that observed in $GtE226^{+/+}$(ic) (Fig. 3*C*), serial transmission of prions from the CNS of $GtE226^{+/+}$(ip) mice produced a pattern of E226-cervid PrP^{Sc} accumulation in the CNS of $GtE226^{+/+}$(ip-ic) mice that resembled that of $GtE226^{+/+}$(ic) mice (Fig. 5*G*).

CWD Transmission by Cohousing Inoculated with Uninoculated Gt Mice. In light of their efficient responses to peripherally administered CWD prions, we asked whether Gt mice could be used to model contagious transmission, which is the hallmark of CWD in natural hosts (46). Five days after intracerebral inoculation with CWD, $GtE226^{+/+}$(ic) mice were introduced to new cages containing additional uninfected $GtE226^{+/+}$ mice. Disease induction in uninoculated, cohoused $GtE226^{+/+}$ mice, referred to as $GtE226^{+/+}$(ch), was remarkably effective. The mean time to disease of $GtE226^{+/+}$(ic) mice was 238 ± 10 d ($n = 10$), while that of their uninoculated, but cohoused $GtE226^{+/+}$(ch) counterparts was 342 ± 28 d ($n = 7$) ($P \leq 0.001$) (Fig. 4*D*). Histoblotting of whole coronal sections of diseased $GtE226^{+/+}$(ch) mice (Fig. 5*H*)

Table 2. Susceptibility of Gt mice expressing deer or elk PrP to CWD prions following i.p. or oral inoculation

	Mean incubation times, ±SEM (n/n_o)				
	GtE226$^{+/+}$(ip)	GtE226$^{+/+}$(ip-ic)	GtQ226$^{+/+}$(ip)	GtE226$^{+/+}$(po)	GtQ226$^{+/+}$(po)
Inoculum	Primary	Secondary			
Elk CWD					
99W12389	308 ± 15 (8/8)	192 ± 7 (8/8)	309 ± 43 (5/5)	328 ± 13 (7/8)	452 ± 26 (4/4)
01-0306	337 ± 1 (9/9)				
04-0306	321 ± 4 (9/9)		413 ± 6 (5/5)	574 ± 36 (3/4)	408 ± 7 (3/3)
012-09442	320 ± 3 (7/7)				
Deer CWD					
D10	301 ± 4 (8/8)		381 ± 12 (6/6)	313 ± 16 (4/4)	436 ± 45 (4/4)
Db99	308 ± 4 (10/10)		363 ± 17 (6/6)	317 ± 7 (3/8)	536 ± 29 (7/7)
978-24384	312 ± 4 (7/7)				
Total CWD	315 ± 3 (58/58)		367 ± 13 (22/22)	366 ± 26 (17/24)	474 ± 19(18/18)

Time to disease onset (incubation time) is expressed as the mean time, in days, at which inoculated mice first developed ultimately progressive signs of neurological disease. Variance is expressed as ±SEM. n/n_o, number of diseased mice/number of inoculated mice. Mice dying of unrelated intercurrent illnesses were excluded from these calculations. Primary refers to passage of CWD isolates to Gt mice by intraperitoneal challenge; secondary refers to serial passage of prions in brain homogenates of diseased mice to mice of the same genetic constitution by intracerebral challenge.

revealed that E226-cervid PrP^{Sc} was diffusely, and bilaterally symmetrically distributed in cortical, thalamic, and hypothalamic regions, in a pattern that was reminiscent of E226-cervid PrP^{Sc} in the brains of GtE226$^{+/+}$(ic) mice receiving E226 CWD prions (Fig. 3 *C* and *D*).

Discussion

Notwithstanding the considerable advantages of Tg mouse models for studying prions, including the capacity to decrease incubation times by transgene overexpression (13), the inability to control random integration of transgene arrays of variable copy number at undefined genomic locations complicates the interpretation of certain analyses, in particular comparative studies designed to assess the effects of PrP primary structural differences on prion pathogenesis. Here we describe the production and initial characterization of two Gt mouse models expressing the PrP coding sequences of elk and deer, which differ only at residue 226. We draw three overarching conclusions from our studies: first, replacement of the coding sequence for mouse PrP with that of deer or elk PrP renders the resulting Gt mice susceptible to CWD prions; second, amino acid variation at residue 226 of deer and elk PrP controls the tempo of disease onset, as well as the targeted accumulation and conformational properties of the resulting prions, reflecting the section and propagation of distinct cervid prion strains; and third, Gt mice offer an unprecedented means to address distinctive aspects of peripheral CWD pathogenesis and contagious transmission that were not afforded by previous Tg mouse models.

Gt Mice Are Susceptible to Cervid Prions. Our findings detailing uniform susceptibility, and relatively rapid responses of GtE226$^{+/+}$ and GtQ226$^{+/+}$ mice to elk and deer CWD prions, stand in contrast to the behaviors of previously produced gene targeted mice designed to abrogate species barriers to bovine and human prions. While expression of bovine PrP^{C} conferred susceptibility to BSE prions in Tg mice, even when the level of bovine PrP^{C} expression was lower than that normally found in the brains of cattle (29–31), counterpart Gt mice were paradoxically less susceptible to BSE than wild-type mice (32, 33). Similarly, despite repeated examples of high susceptibility and rapid incubation times of human prions in Tg mice, even at wild-type levels of human PrP^{C} expression (14, 34–36), counterpart Gt mice exhibited longer vCJD prion incubation times compared with wild-type mice (32), as well as prolonged incubation periods and incomplete attack rates in response to sporadic CJD prions (37). The discrepant susceptibilities of these Tg mice and their Gt equivalents were puzzling because they appeared to undermine the primacy of PrP sequence homology in the control of prion transmission barriers (38). In contrast, the differences we observed in incubation times between CWD-susceptible Tg and Gt mice were surprisingly modest. When the effects of residue 226 on the kinetics of disease onset are considered, our findings in Tg and Gt mice expressing cervid PrP confirm the longstanding inverse relationship between levels of CNS PrP^{C} expression and prion incubation times following intracerebral challenge (13).

Our findings and conclusions make it difficult to reconcile the poor responses of previously produced Gt mice to bovine and

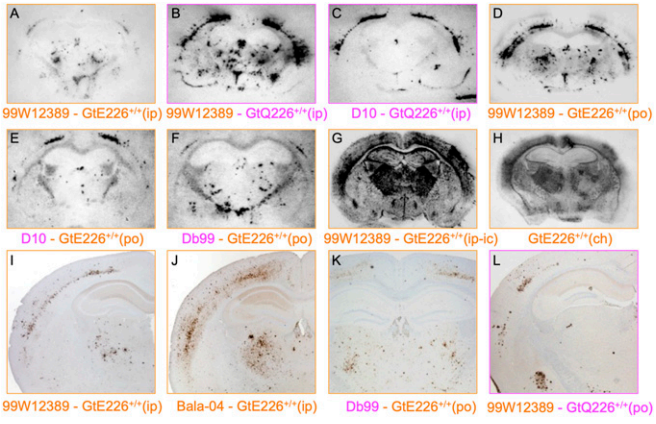

Fig. 5. PrP^{Sc} distribution in brains of diseased Gt mice following peripheral challenges with CWD prions. Coronal sections through the hippocampus and thalamus are shown in all cases. (*A–H*) PK-treated histoblots probed with mAb PRC5. (*I–L*) Immunohistochemical analysis with Fab D18. (Magnification: 2×.) GtE226$^{+/+}$ (orange) or GtQ226$^{+/+}$ mice (magenta) were inoculated either intraperitoneally (ip) or by oral gavage (po) as indicated with either elk (orange) or deer (magenta) CWD isolates. Ip-ic, secondary transmission by the intracerebral route of brain homogenates from ip challenged mice. Ch, uninoculated GtE226$^{+/+}$ mice cohoused with ic-challenged GtE226$^{+/+}$ mice.

human prions on the basis of transgene expression alone, and force consideration of several alternate possibilities. First, the likelihood that the relatively facile responses of GtE226 and GtQ226 mice to prion infection are reflective of unusually virulent properties of CWD prions seems remote given that Gt mice were also equally susceptible to cervid-adapted sheep SSBP/1 and cervid-adapted mouse RML prions (Table 1). Second, previously produced Gt mice were generated on a 129 mouse background (32, 37), while the Gt mice reported here were generated using FVB. Whether the discrepant properties of Gt mice result from the effects of mouse genetic backgrounds can be resolved by studying the outcomes of inbreeding Gt mice onto a 129 background, and correspondingly by repeated backcrossing of bovine and human PrP Gt mice with FVB mice. Third, while GtE226 and GtQ226 mice express elk and deer PrP coding sequences, respectively, previously produced Gt mice were engineered to express chimeric mouse–bovine and mouse–human coding sequences, where the signal peptides of the expressed transgenes originated from mouse PrP (32, 37, 47). While such arrangements are not expected to affect the primary structures of mature bovine and human PrP after signal peptidase cleavage and processing, it is nonetheless well established that amino acid substitutions in signal peptide sequences have a considerable impact on PrP-mediated neurodegeneration by affecting the production of a trapped transmembrane isoform of PrP termed ^{Ctm}PrP (48). Additional studies highlight the unpredictable effects of expressing chimeric PrP constructs on disease outcomes. While Gt mice, referred to as Ki-ChM, expressing a chimeric mouse–human PrP coding sequence containing the mouse PrP signal peptide—as well as mouse PrP sequences at the C terminus—had variable responses to human prions, certain CJD isolates produced disease with mean incubation times in the range of ∼140–180 d (49, 50). When transmitted to Gt mice expressing a different chimeric mouse–human PrP where only the signal peptide is derived from mouse PrP, referred to as Ki-Hu129M/M, mean incubation times of CJD prions that induced disease in Ki-ChM within ∼150 d were prolonged by >300 d (47). With these considerations in mind, and in light of the results reported here, it appears that expression of wild-type human or bovine PrP coding sequences affords the best prospect of conferring susceptibility to CJD and BSE prions in Gt mice.

Cervid PrP Residue 226 Dictates the Propagation of Distinct Strain Conformers. The use of a Gt approach allowed us to unequivocally ascertain the effects of amino acid differences at codon 226 of deer and elk PrP on CWD pathogenesis. Because GtE226$^{+/+}$ and GtQ226$^{+/+}$ mice (and for that matter GtE226$^{+/-}$ and GtQ226$^{+/-}$ mice) produce equivalent amounts of elk and deer PrP^{C}, and because they are otherwise syngeneic, the consistently different kinetics of CWD onset can be unambiguously ascribed to the effects of amino acid variation at residue 226. Our findings also demonstrate that Gt mice are susceptible not only to CWD prions, but also to experimentally adapted cervid prions, including cervid-adapted SSBP/1 and cervid-adapted RML, with variable kinetic effects of the residue 226 dimorphism. The production of Gt mice on an FVB background, and the availability of PrP knockout and previously produced Tg mice on the equivalent inbred mouse background, provided the added advantage of allowing us to compare the effects of residue 226 over a range of transgene expression in a controlled genetic context. The consistently more rapid time to clinical disease in mice expressing elk PrP^{C} compared with their Gt and Tg counterparts expressing deer PrP^{C} across a spectrum of transgene expression emphasizes the impact of residue 226 on CWD. Indeed, the comparative analyses of Tg and Gt mice reported here confirms that the variable responses of Tg5037$^{+/-}$ and Tg1536$^{+/-}$ mice to CWD prions originally reported in limited transmission studies (25), resulted from effects of amino acid differences at residue 226 rather than uncontrolled artifacts of transgene expression.

Our findings are in accordance with the notion that residue 226 in elk and deer PrP^{C} acts to select and propagate distinct strains from an ensemble of PrP^{Sc} conformers by a mechanism that is compatible with the conformational selection model (19). In support of this view, GtE226$^{+/+}$ and GtQ226$^{+/+}$ mice have distinct times to disease onset and neuropathological outcomes in response to intracerebral challenge with the same CWD prion inocula, and the resulting E226 and Q226 prions produced in Gt mice have distinct conformational properties. These findings raise the possibility that the strain properties of CWD prions produced in diseased elk are distinct from those of prions causing CWD in deer. Limited analyses showing distinct pathogenic outcomes between CWD-affected deer and elk (51, 52) are consistent with this interpretation. In light of the influence of strain properties on interspecies prion transmission, our findings that elk and deer PrP^{C} select and propagate different strains are relevant when considering the risk of interspecies CWD transmission, in particular when considering the barrier controlling human susceptibility.

Of note, the effects of amino acid differences at residue 226 on the biological and biochemical properties of CWD prions reported here are supported by structural investigations showing that the distal region of α-helix 3, which contains residue 226, participates with residues in the β2–α2 loop to form a solvent-accessible discontinuous epitope (53, 54). Our subsequent molecular dynamics analyses (55) indicated that E and Q variations at residue 226, as well as the protective polymorphism at the adjacent residue 225 in deer PrP, affected hydrogen bonding between key residues in the β2–α2 loop that modify the strength of interaction between these subdomains, supporting the notion that the plasticity of this discontinuous epitope modulates the efficiency of PrP^{C} to PrP^{Sc} conversion.

Investigations of Peripheral CWD Pathogenesis and Contagious Transmission in Gt Mice. Replication of CWD prions to high titers in the peripheral lymphoid system and their resultant shedding in excrement and bodily fluids of diseased cervids are considered to be the underlying features contributing to the unparalleled transmission efficiency of CWD (5). Because they are purported to express PrP at physiological levels in all appropriate cell types, Gt mice have been endorsed as ideal models in which to study peripheral pathogenesis of prion diseases (38). Our findings confirm that this is the case. Gt mice offer a refined improvement on previously described Tg models of CWD, and a new application to explore peripheral CWD pathogenesis and contagious spread of CWD prions. Remarkably, GtQ226$^{+/+}$ mice showed no difference in time to disease onset following intraperitoneal or intracerebral challenges with CWD (Fig. 4*B*). In contrast, despite robust PrP over expression in the CNS of Tg1536$^{+/-}$ mice (24), which resulted in more rapid times to disease following intracerebral challenge than counterpart GtQ226$^{+/+}$(ic) mice expressing physiological levels of PrP, the response of Tg1536$^{+/-}$ mice to intraperitoneal challenge with CWD prions was highly inefficient, reflected in prolonged times to disease onset compared with GtQ226$^{+/+}$(ip) mice (Fig. 4*C*). We interpret this to mean that the cos.SHaTet cosmid used to create Tg1536$^{+/+}$ mice (24) failed to reconstitute appropriate PrP expression in all compartments required for effective peripheral pathogenesis. In accordance with this interpretation, while spleens of diseased GtQ226$^{+/+}$ mice accumulated PrP^{Sc} following either intracerebral or intraperitoneal inoculation, PrP^{Sc} was undetectable by Western blotting in spleens of diseased Tg1536$^{+/+}$ mice that were challenged by the intracerebral or intraperitoneal route (Fig. 4*G*).

We also show that the route of CWD prion inoculation elicited a pronounced effect on the distribution of cervid PrP^{Sc}-containing lesions in the CNS of Gt mice. Accordingly, while intracerebral inoculation of GtE226$^{+/+}$ mice with 99W12389 CWD

prions resulted in widespread, diffuse, and bilaterally symmetrical PrP^{Sc} deposition in cortical, hippocampal, thalamic, and hypothalamic regions (Fig. 3), the pattern of E226-cervid PrP^{Sc} deposition in $GtE226^{+/+}$ mice challenged intraperitoneally with the same CWD prions was different from, and more restricted than in $GtE226^{+/+}$(ic) mice (Fig. 5). Interestingly, when prions from the brains of these mice were serially passaged to additional $GtE226^{+/+}$ mice by intracerebral inoculation, the pattern of cervid PrP^{Sc} deposition in these $GtE226^{+/+}$(ip-ic) mice reverted to that seen in $GtE226^{+/+}$ mice intracerebrally challenged with 99W12389 (Fig. 5*G*). These findings are consistent with the results of previous findings in wild-type mice infected with experimentally adapted scrapie prions, which showed that route of administration affected the profile of neuropathological lesions (56), and underscore the importance of inoculation route when defining prion strain properties. In light of their highly efficient responses to peripherally administered prions, we reasoned that Gt mice might provide an effective means to model horizontal CWD transmission. Our preliminary findings show Gt mice to be a tractable experimental model in which to ascertain the underlying basis for the remarkably contagious transmission of CWD prions (46).

In conclusion, the Gt mice described here represent an important resource with which to address multiple unresolved issues relating to CWD. Our findings describing the role of amino acid differences at residue 226 of deer and elk PrP in dictating the species-specific selection and propagation of cervid prion strains has important implications for assessing the zoonotic potential of established, as well as newly emergent forms of CWD. Of immediate significance, the origins of CWD in Europe (10, 11), and for that matter North American CWD, are enigmatic, and the relationship, if any, between CWD prions from these locations is currently unclear. Understanding whether residue 226 plays a role in the selection and propagation of novel emergent strains in this context would appear to be of particular importance. While prions causing CWD in South Korea are considered to be derivative of North American CWD (7, 8), whether the properties of these CWD prions were altered as a result of passage through indigenous cervid species also remains to be determined. Comparing the properties of North American, European, and Asian CWD prions using Gt mice represents an important first step to assess the prospect of novel global CWD epidemics with unpredictable ecological and public health consequences. Finally, the refined strategies for PrP gene replacement reported here suggest opportunities for improved Gt mouse models in which to study aspects of human and animal prion biology that have until now not been possible using conventional Tg approaches. The generation of optimized Gt mice expressing human PrP rather than chimeric mouse–human PrP constructs would appear to be of particular importance in this regard.

Materials and Methods

Detailed descriptions of the methods and materials used for the production and characterization of Gt mice, including RNA extraction and analysis by qRT-PCR; prion transmission studies; analyses of PrP^{C} and PrP^{Sc} by Western blotting, histoblotting and IHC; and analysis of the conformational stability of PK-resistant PrP^{Sc} by GdnHCl denaturation are included in *SI Appendix*. Production and characterization of $Tg1536^{+/+}$ and $Tg5037^{+/+}$ mice has been described previously (24, 25). All procedures used in this study were performed in compliance with the Colorado State University Institutional Animal Care and Use Committee.

1. R. G. Will *et al*., A new variant of Creutzfeldt-Jakob disease in the UK. *Lancet* **347**, 921–925 (1996).
2. S. L. Benestad, G. C. Telling, Chronic wasting disease: An evolving prion disease of cervids. *Handb. Clin. Neurol.* **153**, 135–151 (2018).
3. E. S. Williams, S. Young, Chronic wasting disease of captive mule deer: A spongiform encephalopathy. *J. Wildl. Dis.* **16**, 89–98 (1980).
4. M. W. Miller *et al*., Epizootiology of chronic wasting disease in free-ranging cervids in Colorado and Wyoming. *J. Wildl. Dis.* **36**, 676–690 (2000).
5. K. A. Davenport *et al*., Comparative analysis of prions in nervous and lymphoid tissues of chronic wasting disease-infected cervids. *J. Gen. Virol.* **99**, 753–758 (2018).
6. M. W. Miller, E. S. Williams, N. T. Hobbs, L. L. Wolfe, Environmental sources of prion transmission in mule deer. *Emerg. Infect. Dis.* **10**, 1003–1006 (2004).
7. H. J. Sohn *et al*., A case of chronic wasting disease in an elk imported to Korea from Canada. *J. Vet. Med. Sci.* **64**, 855–858 (2002).
8. T. Y. Kim *et al*., Additional cases of chronic wasting disease in imported deer in Korea. *J. Vet. Med. Sci.* **67**, 753–759 (2005).
9. Y. H. Lee *et al*., Experimental chronic wasting disease in wild type VM mice. *J. Vet. Med. Sci.* **75**, 1107–1110 (2013).
10. S. L. Benestad, G. Mitchell, M. Simmons, B. Ytrehus, T. Vikøren, First case of chronic wasting disease in Europe in a Norwegian free-ranging reindeer. *Vet. Res.* **47**, 88 (2016).
11. L. Pirisinu *et al*., Novel type of chronic wasting disease detected in moose (Alces alces), Norway. *Emerg. Infect. Dis.* **24**, 2210–2218 (2018).
12. S. B. Prusiner, "Prions (Les Prix Nobel Lecture)" in *Les Prix Nobel*, T. Frängsmyr, Ed. (Almqvist & Wiksell International, Stockholm, Sweden, 1998), pp. 268–323.
13. S. B. Prusiner *et al*., Transgenetic studies implicate interactions between homologous PrP isoforms in scrapie prion replication. *Cell* **63**, 673–686 (1990).
14. G. C. Telling *et al*., Prion propagation in mice expressing human and chimeric PrP transgenes implicates the interaction of cellular PrP with another protein. *Cell* **83**, 79–90 (1995).
15. M. Bruce *et al*., Transmission of bovine spongiform encephalopathy and scrapie to mice: Strain variation and the species barrier. *Philos. Trans. R. Soc. Lond. B Biol. Sci.* **343**, 405–411 (1994).
16. G. C. Telling, Transgenic mouse models and prion strains. *Top. Curr. Chem.* **305**, 79–99 (2011).
17. R. A. Bessen, R. F. Marsh, Distinct PrP properties suggest the molecular basis of strain variation in transmissible mink encephalopathy. *J. Virol.* **68**, 7859–7868 (1994).
18. G. C. Telling *et al*., Evidence for the conformation of the pathologic isoform of the prion protein enciphering and propagating prion diversity. *Science* **274**, 2079–2082 (1996).
19. J. Collinge, A. R. Clarke, A general model of prion strains and their pathogenicity. *Science* **318**, 930–936 (2007).
20. J. Bian *et al*., Prion replication without host adaptation during interspecies transmissions. *Proc. Natl. Acad. Sci. U.S.A.* **114**, 1141–1146 (2017).
21. J. D. Wadsworth *et al*., Human prion protein with valine 129 prevents expression of variant CJD phenotype. *Science* **306**, 1793–1796 (2004).
22. L. Cervenáková, R. Rohwer, S. Williams, P. Brown, D. C. Gajdusek, High sequence homology of the PrP gene in mule deer and Rocky Mountain elk. *Lancet* **350**, 219–220 (1997).
23. S. Kaluz, M. Kaluzova, A. P. Flint, Sequencing analysis of prion genes from red deer and camel. *Gene* **199**, 283–286 (1997).
24. S. R. Browning *et al*., Transmission of prions from mule deer and elk with chronic wasting disease to transgenic mice expressing cervid PrP. *J. Virol.* **78**, 13345–13350 (2004).
25. R. C. Angers *et al*., Chronic wasting disease prions in elk antler velvet. *Emerg. Infect. Dis.* **15**, 696–703 (2009).
26. R. C. Angers *et al*., Prion strain mutation determined by prion protein conformational compatibility and primary structure. *Science* **328**, 1154–1158 (2010).
27. A. Le Dur *et al*., Divergent prion strain evolution driven by PrP^{C} expression level in transgenic mice. *Nat. Commun.* **8**, 14170 (2017).
28. R. C. Moore *et al*., Mice with gene targetted prion protein alterations show that *Prnp*, *Sinc* and *Prni* are congruent. *Nat. Genet.* **18**, 118–125 (1998).
29. M. R. Scott *et al*., Identification of a prion protein epitope modulating transmission of bovine spongiform encephalopathy prions to transgenic mice. *Proc. Natl. Acad. Sci. U.S.A.* **94**, 14279–14284 (1997).
30. A. Buschmann, M. H. Groschup, Highly bovine spongiform encephalopathy-sensitive transgenic mice confirm the essential restriction of infectivity to the nervous system in clinically diseased cattle. *J. Infect. Dis.* **192**, 934–942 (2005).
31. J. Castilla *et al*., Early detection of PrPres in BSE-infected bovine PrP transgenic mice. *Arch. Virol.* **148**, 677–691 (2003).
32. M. T. Bishop *et al*., Predicting susceptibility and incubation time of human-to-human transmission of vCJD. *Lancet Neurol.* **5**, 393–398 (2006).
33. M. E. Bruce *et al*., Transmissions to mice indicate that 'new variant' CJD is caused by the BSE agent. *Nature* **389**, 498–501 (1997).
34. E. A. Asante *et al*., BSE prions propagate as either variant CJD-like or sporadic CJD-like prion strains in transgenic mice expressing human prion protein. *EMBO J.* **21**, 6358–6366 (2002).
35. Q. Kong *et al*., Chronic wasting disease of elk: Transmissibility to humans examined by transgenic mouse models. *J. Neurosci.* **25**, 7944–7949 (2005).
36. V. Béringue *et al*., Prominent and persistent extraneural infection in human PrP transgenic mice infected with variant CJD. *PLoS One* **3**, e1419 (2008).
37. M. T. Bishop, R. G. Will, J. C. Manson, Defining sporadic Creutzfeldt-Jakob disease strains and their transmission properties. *Proc. Natl. Acad. Sci. U.S.A.* **107**, 12005–12010 (2010).
38. E. Cancellotti *et al*., The role of host PrP in transmissible spongiform encephalopathies. *Biochim. Biophys. Acta* **1772**, 673–680 (2007).
39. K. M. Green *et al*., The elk PRNP codon 132 polymorphism controls cervid and scrapie prion propagation. *J. Gen. Virol.* **89**, 598–608 (2008).

40. K. M. Green *et al*., Accelerated high fidelity prion amplification within and across prion species barriers. *PLoS Pathog.* **4**, e1000139 (2008).
41. P.-M. Lledo, P. Tremblay, S. J. DeArmond, S. B. Prusiner, R. A. Nicoll, Mice deficient for prion protein exhibit normal neuronal excitability and synaptic transmission in the hippocampus. *Proc. Natl. Acad. Sci. U.S.A.* **93**, 2403–2407 (1996).
42. D. Peretz *et al*., Strain-specified relative conformational stability of the scrapie prion protein. *Protein Sci.* **10**, 854–863 (2001).
43. A. Taraboulos *et al*., Regional mapping of prion proteins in brain. *Proc. Natl. Acad. Sci. U.S.A.* **89**, 7620–7624 (1992).
44. R. H. Kimberlin, C. A. Walker, Pathogenesis of scrapie (strain 263K) in hamsters infected intracerebrally, intraperitoneally or intraocularly. *J. Gen. Virol.* **67**, 255–263 (1986).
45. M. Prinz *et al*., Oral prion infection requires normal numbers of Peyer's patches but not of enteric lymphocytes. *Am. J. Pathol.* **162**, 1103–1111 (2003).
46. M. W. Miller, E. S. Williams, Prion disease: Horizontal prion transmission in mule deer. *Nature* **425**, 35–36 (2003).
47. A. Kobayashi, M. Asano, S. Mohri, T. Kitamoto, Cross-sequence transmission of sporadic Creutzfeldt-Jakob disease creates a new prion strain. *J. Biol. Chem.* **282**, 30022–30028 (2007).
48. N. S. Rane, O. Chakrabarti, L. Feigenbaum, R. S. Hegde, Signal sequence insufficiency contributes to neurodegeneration caused by transmembrane prion protein. *J. Cell Biol.* **188**, 515–526 (2010).
49. Y. Taguchi, S. Mohri, J. W. Ironside, T. Muramoto, T. Kitamoto, Humanized knock-in mice expressing chimeric prion protein showed varied susceptibility to different human prions. *Am. J. Pathol.* **163**, 2585–2593 (2003).
50. T. Kitamoto *et al*., Follicular dendritic cell of the knock-in mouse provides a new bioassay for human prions. *Biochem. Biophys. Res. Commun.* **294**, 280–286 (2002).
51. B. L. Race *et al*., Levels of abnormal prion protein in deer and elk with chronic wasting disease. *Emerg. Infect. Dis.* **13**, 824–830 (2007).
52. E. S. Williams, S. Young, Neuropathology of chronic wasting disease of mule deer (Odocoileus hemionus) and elk (Cervus elaphus nelsoni). *Vet. Pathol.* **30**, 36–45 (1993).
53. D. R. Pérez, F. F. Damberger, K. Wüthrich, Horse prion protein NMR structure and comparisons with related variants of the mouse prion protein. *J. Mol. Biol.* **400**, 121–128 (2010). Erratum in: *J. Mol. Biol.* **402**, 929–930 (2010).
54. B. Christen, S. Hornemann, F. F. Damberger, K. Wüthrich, Prion protein NMR structure from tammar wallaby (Macropus eugenii) shows that the beta2-alpha2 loop is modulated by long-range sequence effects. *J. Mol. Biol.* **389**, 833–845 (2009).
55. R. Angers *et al*., Structural effects of PrP polymorphisms on intra- and interspecies prion transmission. *Proc. Natl. Acad. Sci. U.S.A.* **111**, 11169–11174 (2014).
56. G. W. Outram, H. Fraser, D. T. Wilson, Scrapie in mice. Some effects on the brain lesion profile of ME7 agent due to genotype of donor, route of injection and genotype of recipient. *J. Comp. Pathol.* **83**, 19–28 (1973).
57. H. E. Kang *et al*., Characterization of conformation-dependent prion protein epitopes. *J. Biol. Chem.* **287**, 37219–37232 (2012).